ARTICLES

Endohedral Cluster of Li$_{10}$O with T_d Symmetry

Jesús Centeno,*,† **Renato Contreras,***,‡ **and Patricio Fuentealba***,†

Departamento de Física, and Departamento de Química, Facultad de Ciencias, Universidad de Chile, Las Palmeras 3425, Santiago de Chile, Chile

A detailed numerical study of several isomers of the Li$_{10}$ cluster has been done. The analysis of the electronic localization function and the analysis of energy diagrams revealed the existence of one cluster with an inner space capable to suit a heteroatom. The perfect candidate is the Li$_{10}$O cluster due to the experimental evidence of the [Li$_6$O]$^{4+}$ core, the same core present in Li$_{10}$O. In order to check the thermodynamic stability of this cluster, an analysis of its dissociation channels has been done. The IR and UV−vis spectra have been calculated to help in the further identification of this new cluster.

Introduction

Designing novel chemically stable clusters has become more important as a part of the strategy to make nanostructured materials. Since the discovery of the shell structure in the alkali metal clusters,[1] the theoretical and experimental study of them has led to a good understanding of their fundamental properties. Among them, lithium clusters are the most studied. Lithium is the lightest element that is metallic under normal conditions and, because of having only three electrons, is computationally less demanding to study than the other alkali atoms. It has only one single s valence electron and the energy hypersurface of their clusters present many flat minima and no tendency to form directional bonding as the elements with p and d electrons. More recently, several works have studied binary clusters. In particular, there have been some studies of clusters formed by mono- or divalent metallic elements combined with a more electronegative element. Examples are Cs$_n$O$_m$,[2] Li$_n$H$_m$,[3,4] Mg$_n$O$_m$,[5] and Ca$_n$O$_m$.[6] All of them are dominated by stoichiometric ionic bonding and, in some cases, segregation takes place into a purely ionic localized part and a metallic delocalized part.

In this work, we will concentrate in a particular lithium oxide cluster, Li$_{10}$O. The first experimental evidence of a lithium oxide cluster was the Li$_3$O system discovered by Wu et al.[7] The same research group confirmed later the existence[8] of Li$_4$O and Li$_5$O. On a different line, the [Li$_6$O]$^{4+}$ ion has been found as a core of a dilithium phosphanediide with a perfect O_h symmetry.[9] The same core has been also found in a lithium-benzamidinates crystals.[10] However, the neutral Li$_6$O cluster has not been isolated and calculations predicted a D_{3d} symmetry.[11] In all of these systems, the octet rule for second period elements is not followed, and the term "hypervalent oxygen" has been coined. Indeed, early calculations by Schleyer et al.[12] predicted that lithium oxide clusters have the oxygen atom located in the center and that these clusters are thermodynamically stable with respect to the loss of a lithium molecule or a lithium atom. Oxygen

being more electronegative localizes two electrons of the lithium atoms skeleton, and the two positive charges are distributed among the lithium atoms. Hence, the geometry should be such as to alleviate the electrostatic repulsion contributing to the thermodynamic stability. Jones et al.[13] have done a computational study of Li$_n$ ($n = 2−10$) and Li$_n$O ($n = 1−9$) clusters, and Bonačić- Koutecký et al.[14] have studied the small members of the series Li$_n$O ($n = 3,4$). The hyperlithium molecules have been studied by Schleyer and co-workers.[12,15] They signed out the importance of these systems to understand the new class of nonstoichiometric molecules. Experimentally, the lithium oxide family of clusters has been produced by a laser vaporization source and the ionization potentials have been measured.[16−18] The ionization potentials measured in ref 17 show clearly a maximum at Li$_6$O and Li$_{10}$O which have been nicely explained by the shell model.

However, as far as we know, the cluster Li$_{10}$O, the subject of this work, has not been, in a detailed way, studied before. In a systematic study[19] of pure alkali metal clusters, we found a special Li$_{10}$ cluster with a perfect tetrahedral, T_d, geometry, which is approximately 15.0 kcal/mol higher in energy than the most stable one. This T_d cluster represents a perfect pyramid. The importance of being tetrahedral has been emphasized before. Pyykkö has found a whole series of tetrahedral cadmium clusters.[20] A tetrahedral Au$_{20}$ cluster has been isolated experimentally,[21] and later it has been observed in solution, coordinated with eight PPh$_3$ (Ph = phenyl) ligands[22] and a bipyramidal Al$_{30}$ cluster has also been proposed.[23] This prompted us to take a careful looking at the properties of the pyramidal Li$_{10}$. It was found that it has a negative charge of almost two electrons at the center of the pyramid. Further, the electronic configuration is a$_1^2$t$_2^6$a$_1^2T_d^2T_d^2T_d^2$a$_1^2$ which suggests that taking out two electrons a closed shell will appear opening the band gap and increasing the stability. Hence, in this work, the possible stability of a cluster with an oxygen atom at the center of the structure, the Li$_{10}$O cluster, is proposed.

* Corresponding author. E-mail: jesus@fisica.ciencias.uchile.cl (J.C.), rcontrer@uchile.cl (R.C.), and pfuentea@uchile.cl (P.F.).
† Departamento de Física.
‡ Departamento de Química.

Computational Details

The geometry optimization of the set of Li_{10} and Li_nO clusters were performed using the Kohn–Sham method and the B3LYP hybrid functional[24–27] with the polarized split-valence basis set 6-311++G(3df,3pd)[28–33] using the Gaussian03 package.[34] A vibrational analysis was performed to discriminate between minima and transition states in the potential energy surface and confirm the stability of the structures. To calibrate the accuracy of the results, most of the calculations were also done with the B3PW91 functional and also using a small basis set without finding significant differences. For the most important clusters, Li_{10} and $Li_{10}O$, CCSD(T)/6-311++G(d) single point calculations at the B3LYP optimized geometry have been done. Natural population analysis (NPA) was performed using the Gaussian03 implementation of the NBO program.[35] The topological analysis of ELF[36–38] was done using the TOPMOD package,[39] the ELF's isosurfaces and molecular graphics images were produced using the UCSF Chimera[40] and PyMOL[41] packages. The ELF is defined[36] in terms of the excess of local kinetic energy density due to the Pauli exclusion principle,

$$ELF = \left[1 + \left(\frac{D}{D_h}\right)^2\right]^{-1} \quad (1)$$

where D is expressed in terms of the local kinetic energy density, T_s, of the actual noninteracting fermionic system, and the von Weizsäcker functional, T_W,

$$D = T_s - T_W, \; T_s = \frac{1}{2}\sum_i |\nabla\varphi_i|^2, \; T_W = \frac{1}{8}\frac{|\nabla\rho|^2}{\rho} \quad (2)$$

and D_h is the kinetic energy density of a homogeneous electron gas with a density equal to the local density,
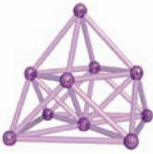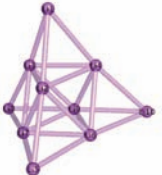
$$D_h = C_F \rho^{5/3} \quad (3)$$

where C_F is the Fermi constant. The ELF can take values in the range of 0 to 1, with 1 corresponding to a perfect localization (i.e., antiparallel spin electron pair or single electron picture) and 0.5 corresponding to a perfect delocalization (a situation analogous to that of the homogeneous electron gas, i.e., jellium model). From this approach, it is clear that the ELF can be used to study the bonding nature and electron behavior on different regions of a cluster.[42–44]

Results and Discussion

The main geometric parameters and relatives energies at B3LYP/6-311++G(3df,3pd), B3LYP/6-311++G(d), and CCSD(T)/6-311++G(d) levels of Li_{10} clusters are shown in Table 1. The D_{2d} isomer is the most stable followed very close in energy by the C_s. The C_{4v} and the T_d isomers are higher in energy by about 13 and 15 kcal/mol, respectively. It is important to note that the T_d cluster has not been proposed before. Moreover, the T_d cluster is the most compact one. The average distance among neighbor atoms is the shortest.

In the study of Li_{10} clusters, we found that, out of the four isomers, three of them (D_{2d}, C_{4v}, and T_d) present an inner "empty" space in their structures capable of suit one heteroatom in order to form a cage-like cluster. The ELF analysis, using an isosurface of 0.85 (Figure 1), shows that the T_d cluster is the best choice because it is the only one with a basin in the center

TABLE 1: Structures, Relative Energies, and Bond Distances of Li_{10} Clusters

Cluster	ΔE (kcal/mol)	Bond Distance (Å)
Li_{10} (D_{2d})	0.0 (a) 0.0 (b) 0.0 (c)	Li_3-$Li_{6,10}$, Li_4-$Li_{6,10}$, Li_2-$Li_{5,8}$, Li_9-$Li_{5,8}$ = 2.852 Li_1-$Li_{3,4}$, Li_7-$Li_{2,9}$ = 3.186; Li_1-$Li_{6,10}$, Li_7-$Li_{5,8}$ = 2.993 Li_2-Li_{10}, Li_3-Li_8, Li_4-Li_5, Li_6-Li_9 = 3.077
Li_{10} (C_s)	2.1 (a) 2.2 (b) 0.6 (c)	Li_1-Li_{10}, Li_2-Li_9 = 3.320; Li_2-Li_{10} = 3.536 Li_6-$Li_{2,10}$ = 2.462; Li_8-$Li_{1,9}$ = 2.495; Li_1-Li_9 = 3.323 Li_5-$Li_{1,9}$ = 3.143; Li_5-$Li_{2,10}$ = 3.179; Li_8-$Li_{4,7}$ = 2.695 Li_6-Li_3 = 2.793; Li_3-$Li_{4,7}$ = 2.830; Li_4-Li_7 = 2.901 Li_3-Li_6 = 3.108; Li_6-$Li_{4,7}$ = 3.162; Li_1-Li_7, Li_4-Li_9 = 3.182 Li_2-Li_4, Li_7-Li_{10} = 3.539; Li_3-$Li_{2,10}$ = 3.196
Li_{10} (C_{4v})	13.5 (a) 13.5 (b) 12.1 (c)	Li_2-$Li_{9,10}$; Li_6-$Li_{9,10}$ = 2.992; Li_1-$Li_{3,7}$; Li_4-$Li_{3,7}$ = 4.421 Li_1-$Li_{2,10}$, Li_3-$Li_{6,10}$, Li_4-$Li_{6,9}$, Li_7-$Li_{2,9}$ = 2.930 Li_8-$Li_{2,6,9,10}$ = 3.062; Li_5-$Li_{1,3,4,7}$ = 3.126 Li_5-$Li_{2,6,9,10}$ = 2.819
Li_{10} (T_d)	15.0 (a) 15.1 (b) 15.0 (c)	Li_2-$Li_{3,4,6,7}$, Li_3-$Li_{4,7,9}$, Li_9-$Li_{4,6,7}$, Li_4-Li_6, Li_6-Li_7 = 2.639 Li_1-$Li_{2,3,4}$, Li_5-$Li_{2,6,7}$, Li_8-$Li_{3,7,9}$, Li_{10}-$Li_{4,6,9}$ = 3.181

[a] B3LYP/6-311++G(3df,3pd). [b] B3LYP/6-311++G(d). [c] CCSD(T)/6-311++G(d).

with a population of two electrons. The other clusters do not show this inner basin. This isomer has four other basins with peaks between atoms in the vertices of the tetrahedral external subunits, with a population of two electrons. The isosurface analysis shows multicentric and multielectronic bonds, of the type four centers, two electrons (4c-2e). The scenario for the isomer D_{2d} is completely different to that of T_d, being characterized by the existence of eight basins with an electronic population roughly between 1.17 and 1.27 electrons. Four of these basins are located in the tetrahedral subunits that are at the top and the bottom of the cluster, and the other four are in the tetrahedral subunits that are part of the interior. The isosurface analysis reveals multicentric bonds, of four centers, containing something more than one electron each one, for inner, upper, and lower bonds. In the C_s isomer, it can also be noted the existence of tetrahedral subunits and three basins, one in the upper tetrahedral subunit, with an electronic population of two electrons, the other in the subunit at the interior with a population of approximately five electrons and the lower one located at the pyramidal subunit with a population of approximately three electrons. The isosurface analysis reveals the existence of three groups of delocalized bonds, 4c-2e, multicentric-5e, and 5c-3e for the upper, interior, and lower subunits, respectively. The C_{4v} isomer presents five basins, with peaks between atoms in the vertices of the tetrahedral external subunits, revealing bonds of the type 4c-2e for each one.

The analysis of the energy diagram (Figure 2) of the Li_{10} isomers supports the choice of the isomer with T_d symmetry since the removal of an electronic pair results in a more stable

Endohedral Cluster of Li$_{10}$O with T_d Symmetry

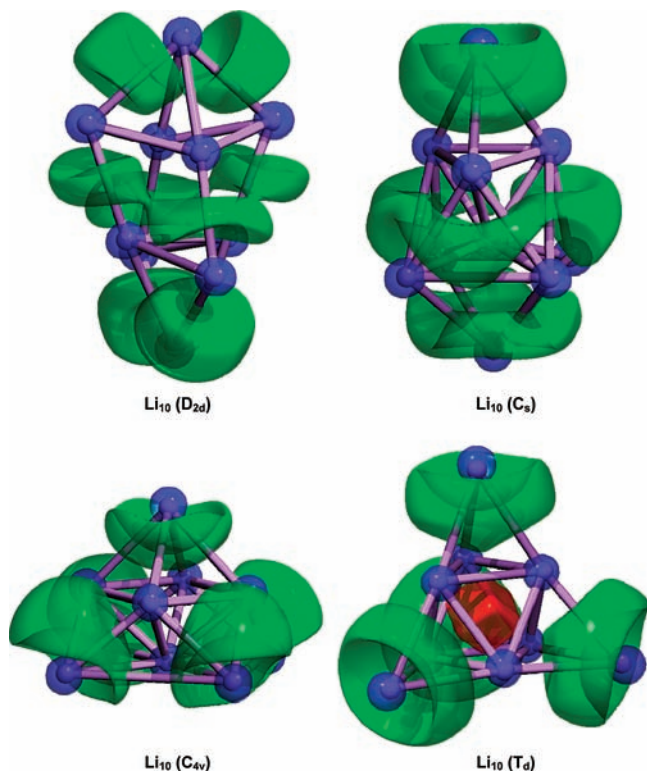*J. Phys. Chem. A, Vol. 113, No. 48, 2009* **13453**

Figure 1. ELF's isosurfaces of Li$_{10}$ clusters.

cation (leading to a state with a triple degenerate frontier molecular orbital) with a gap increase of 1.38 eV. The removal of an electronic pair in the other isomers leads to a double degeneracy for the D_{2d} cluster with a gap increase of 0.13 eV, and a quasidegeneracy in the C_{4v} isomer with a difference of 0.0016 eV between one a_1 and two e orbitals. The gap increase for this isomer is 1.68 eV. In the case of the C_s cluster, the removal of the electronic pair results in a transition state (one imaginary frequency of 12.9i cm^{-1}).

The existence of an inner basin with two electrons and the increase in the gap value when two electrons are removed in the T_d isomer suggests the possibility of the inclusion of an atom capable to take the two "inner" electrons to form a

cage-like cluster. The perfect candidate should be an atom from group VI of the periodic table, since it needs only two electrons to complete their outer shell. We choose the oxygen atom because of the experimental evidence[9] of [Li$_6$O]$^{4+}$, which can be used as a core for the growing of a Li$_{10}$O cluster. The experimental Li—O distances in the [Li$_6$O]$^{4+}$ aggregate are around 1.81—1.90 Å, whereas in our calculations, they are of 1.87 Å, which is in concordance with the experimental values. We ran calculations on Li$_{10}$S, but this cluster has a triple degenerated imaginary frequencies of 81.4i cm^{-1} at B3LYP/6-31G(d) level. Descending in group I of the periodic table, we found that the clusters Na$_{10}$O and K$_{10}$O are stable clusters, despite the fact that according to our calculations there are no Na$_{10}$ and K$_{10}$ clusters with a T_d symmetry, showing the importance of oxygen atom as a stabilizer center.

The main geometric and electronic parameters of Li$_{10}$O are shown in Table 2 in comparison with the ones of Li$_6$O (O_h). As can be seen in Table 1 and Table 2, the distances between Li atoms are the same for both clusters, Li$_{10}$ and Li$_{10}$O, 2.639 Å for horizontal bonds and 3.181 Å for the bonds located at the edges of the tetrahedron, while the distances between the Li atoms and Li and O atoms are 1.9% shorter than in the cluster Li$_6$O. It is remarkable that the inclusion of an oxygen atom inside the Li$_{10}$ cluster does not increase the Li—Li bond distances.

To check whether the Li$_{10}$O T_d was a low-lying isomer, we performed a search using a "Big-Bang"[19,45-48] stochastic search algorithm. In this algorithm, we created 10 000 random configurations of 10 atoms in a highly compressed space, in the order of the molar volume, and then letting these supercompressed structures expand in a process of "explosion", relaxing to the minima of the local surface energy using the semiempirical package MSINDO.[49-51] After this process, there is a selection of those grouped in sets of energy whose differences are lower than 0.17 eV. The structures and relative energies of the Li$_{10}$O clusters found by this approach are reported in Table 3. As can be seen, the T_d isomer is, in fact, a low-lying isomer, with only 5.5 kcal/mol above the most stable one (C_1) at B3LYP/6-311++G(3df,3pd) level, and at CCSD(T)/6-311++G(d) level with only 2.6 kcal/mol,
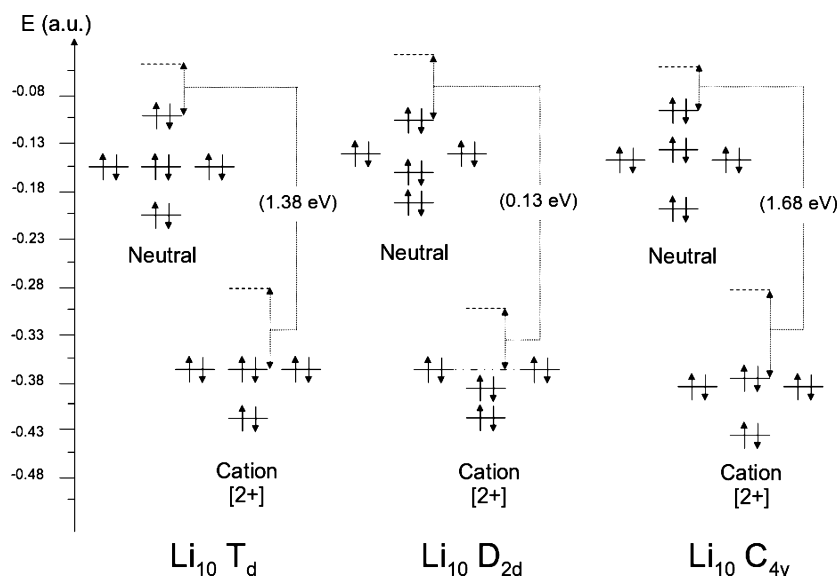

Figure 2. Energy diagram of Li$_{10}$ clusters (neutral and cationic). The dashed line corresponds to the unoccupied states (LUMO). Values between parentheses are the gap increase as a result of the removal of an electronic pair.

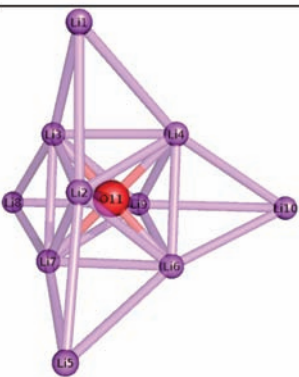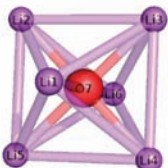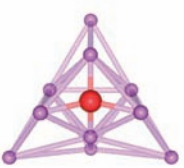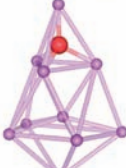**TABLE 2: Structures and Bond Distances of the Li$_{10}$O and Li$_6$O Clusters**
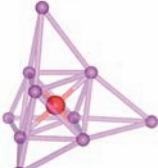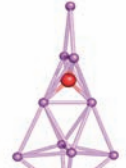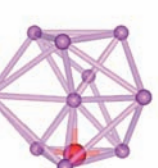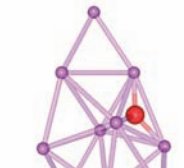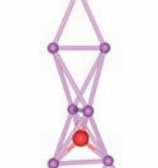
Cluster	Bond Distance (Å)

Li$_{2,3,4,6,7,9}$-O = 1.866

Li$_3$-Li$_{2,4}$, Li$_4$-Li$_6$, Li$_7$-Li$_9$ = 2.639

Li$_1$-Li$_{2,3,4}$, Li$_2$-Li$_5$, Li$_3$-Li$_8$, Li$_4$-Li$_{10}$ = 3.181

Li-O = 1.902

Li-Li = 2.690

TABLE 3: Structures and Relative Energies of Li$_{10}$O Clusters

Li$_{10}$O (C$_1$)
ΔE = 0.0 kcal/mol (a)
ΔE = 0.0 kcal/mol (b)

Li$_{10}$O (C$_s$)
ΔE = 4.9 kcal/mol (a)
ΔE = 4.2 kcal/mol (b)

Li$_{10}$O (T$_d$)
ΔE = 5.5 kcal/mol (a)
ΔE = 2.6 kcal/mol (b)

Li$_{10}$O (C$_{2v}$)
ΔE = 7.7 kcal/mol (a)
ΔE = 6.2 kcal/mol (b)

Li$_{10}$O (C$_{2v}$)
ΔE = 9.0 kcal/mol (a)
ΔE = 10.7 kcal/mol (b)

Li$_{10}$O (C$_1$)
ΔE = 9.7 kcal/mol (a)
ΔE = 7.6 kcal/mol (b)

Li$_{10}$O (C$_1$)
ΔE = 13.5 kcal/mol (a)
ΔE = 13.5 kcal/mol (b)

Li$_{10}$O (C$_1$)
ΔE = 17.1 kcal/mol (a)
ΔE = 17.5 kcal/mol (b)

Li$_{10}$O (C$_{2v}$)
ΔE = 23.2 kcal/mol (a)
ΔE = 24.3 kcal/mol (b)

[a] B3LYP/6-311++G(3df,3pd). [b] CCSD(T)/6-311++G(d).

becoming the second stable one. This energy difference is so small that it is impossible to exclude its presence at room temperature. It is also interesting to take a look at the geometrical and electronic structure of those isomers. Besides the T_d isomer, two of them, the most stable one with C_1

TABLE 4: Dissociation Channels of the Li$_{10}$O (T_d) Cluster

				ΔE (kcal/mol)
Li$_{10}$O (T_d)	→	LiO (D$_{\infty h}$)	+ Li$_9$ (C$_{4v}$)	136.02
Li$_{10}$O (T_d)	→	Li$_2$O (D$_{\infty h}$)	+ Li$_8$ (T_d)	71.19
Li$_{10}$O (T_d)	→	Li$_3$O (D$_{3h}$)	+ Li$_7$ (D$_{5h}$)	47.52
Li$_{10}$O (T_d)	→	Li$_4$O (T_d)	+ Li$_6$ (D$_{4h}$)	35.67
Li$_{10}$O (T_d)	→	Li$_5$O (C$_{2v}$)	+ Li$_5$ (C$_{2v}$)	42.50
Li$_{10}$O (T_d)	→	Li$_6$O (D$_{2d}$)	+ Li$_4$ (D$_{2h}$)	66.35
Li$_{10}$O (T_d)	→	Li$_7$O (C$_s$)	+ Li$_3$ (C$_{2v}$)	42.79
Li$_{10}$O (T_d)	→	Li$_8$O (C$_s$)	+ Li$_2$ (D$_{\infty h}$)	27.08
Li$_{10}$O (T_d)	→	Li$_9$O (C$_{2v}$)	+ Li	26.11

symmetry and the fourth one with C_{2v} symmetry, contain the oxygen atom at the center of the cage structure; see Table 3. Following the electronic shell model, they should also tend to have only eight electrons on the surface. To study them further, the oxygen atom was dropped and the Li$_{10}$ skeleton geometry relaxed. However, they do not correspond to a minimum but a saddle point with one and two imaginary frequencies, respectively. Even though they do not represent a minimum, the ELF of the fixed Li$_{10}$ skeleton was calculated, and only the C_{2v} structure presents a basin at the center of the cage like the T_d isomer. One can note that the T_d and the C_{2v} structures are the only ones with a perfect octahedral Li$_6$ substructure. This great symmetry can explain why the electronic shell model works only for those isomers. It is known that the electronic shell model works much better for the more symmetrical structures. Here, it is then clear that, among all stable isomers of Li$_{10}$, only the one of T_d symmetry presents a basin at the center of the cage.

To study further the possible existence of the Li$_{10}$O cluster, we explored the dissociation channels of Li$_{10}$O. As the ionic oxygen−lithium bond is the strongest one, we studied all of the possibilities of the type Li$_{10}$O → Li$_{10-n}$O + Li$_n$. In order to do that, we first optimized the structures of the Li$_n$ and Li$_{10-n}$O clusters using the same methodology as before.

For Li$_n$, our isomers are similar from those obtained in the calculations by Jones et al.,[13] except in the case of Li$_7$, Li$_8$, Li$_9$, and Li$_{10}$. For Li$_7$, they reported a C_{3v} structure, and in this work, we found a D_{5h} structure as the most stable one, coinciding with the structure reported by Boustani et al.[14] in HF-based calculations. In the case of Li$_8$, Jones et al.[13] reported a D_{5h} structure, whereas we found as the most stable structure the T_d isomer, coinciding, again with the work of Boustani et al.[14] For Li$_9$, they considered it unwise to make a prediction of the most stable isomer; in this work, we report the C_{4v} as the stable structure for this number of Li atoms. In Li$_{10}$ cluster, Jones et al.[13] reported a C_1 isomer; we have found a D_{2d} isomer as the most stable one.

For Li$_n$O, the isomers found in this work agrees more with those found by Lievens et al.[16] than those of Jones et al.,[13] except in the case of Li$_7$O, where they reported a C_{2v} structure and we found a C_s isomer (coinciding with Jones et al.[13]). The structures presented by Viallon et al.[17] are, in general, more symmetric.

The energies associated with all possible dissociation channels are presented in Table 4. In all cases the Li$_{10}$O cluster shows a great stability toward the dissociation in its constituent clusters. The dissociation channels are highly endothermic. Hence, once the cluster is formed, it should be thermodynamic stable.

The natural population analysis (NPA) data for the Li$_{10}$O and the dissociation clusters are summarized in Table 5. The ionic character of the Li−O bond in these clusters is clearly shown. The natural charges for the oxygen atom vary in the

Endoheral Cluster of Li$_{10}$O with T_d Symmetry

J. Phys. Chem. A, Vol. 113, No. 48, 2009 **13455**

TABLE 5: Natural Charges Populations of the Li$_n$O Clusters

n	O	Li$_1$	Li$_2$	Li$_3$	Li$_4$	Li$_5$	Li$_6$	Li$_7$	Li$_8$	Li$_9$	Li$_{10}$
1	−0.95	0.95[a]									
2	−1.91	0.95[a]	0.95[a]								
3	−1.92	0.64[a]	0.64[a]	0.64[a]							
4	−1.94	0.48[a]	0.48[a]	0.48[a]	0.48[a]						
5	−1.92	0.51[a]	0.51[a]	−0.18	0.55[a]	0.55[a]					
6	−1.92	−0.20	0.58[a]	−0.20	0.58[a]	0.58[a]	0.58[a]				
7	−1.93	0.37[a]	−0.03	0.45[a]	0.40[a]	−0.03	0.40[a]	0.37[a]			
8	−1.93	0.41[a]	0.47[a]	0.47[a]	0.41[a]	0.44[a]	−0.07	−0.12	−0.07		
9	−1.92	0.13	0.13	0.47[a]	−0.48	0.13	0.47[a]	0.47[a]	0.47[a]	0.13	
10	−2.03	−0.06	0.38[a]	0.38[a]	0.38[a]	−0.06	0.38[a]	0.38[a]	−0.06	0.38[a]	−0.06

[a] Atoms bonding to O atom.
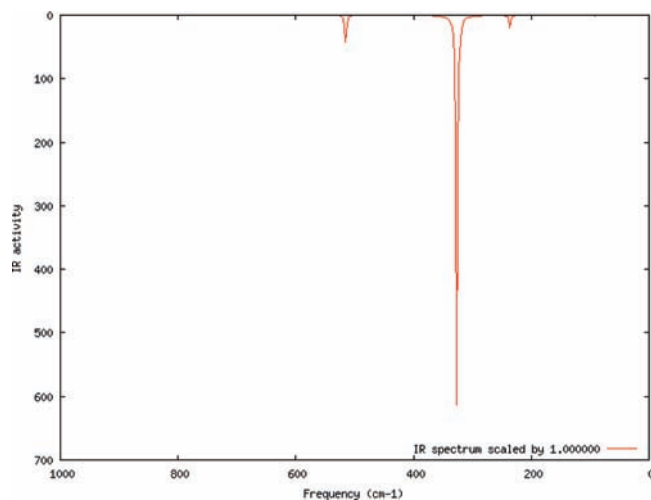
Figure 3. IR spectra of the Li$_{10}$O (T_d) cluster.
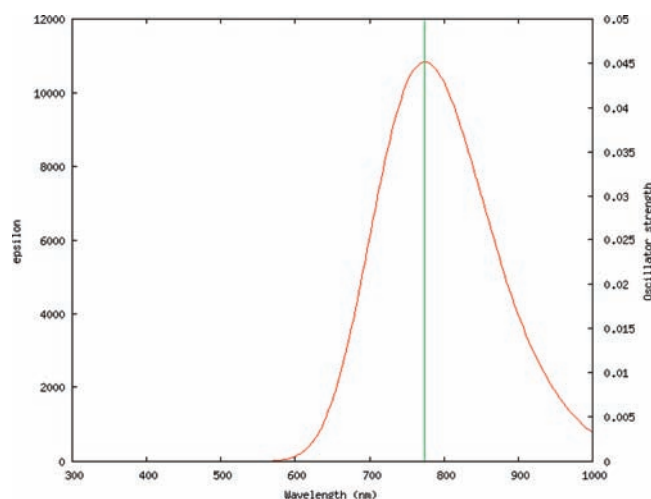
Figure 4. UV–vis spectra of the Li$_{10}$O (T_d) cluster.

range of −0.95 for LiO to −2.03 for Li$_{10}$O, becoming stabilized around −1.9 for the rest of Li$_n$O dissociation products. It is interesting to note the increase in the charge on oxygen atom just for the Li$_{10}$O cluster. The differences in the charge distribution are due to the dependency of charge with the symmetry of the cluster.

The ionization potential constitutes one the most important quantities amenable of experimental measurements. For the lithium oxides family, there are two independent experiments with very similar results.[16,17] The calculations reported here are in reasonable agreement with them. For instance, for Li$_6$O, we calculated an ionization potential of 4.66 eV, whereas the experimental value[17] is of 4.70 eV. For Li$_{10}$O, the calculation

for the most stable isomer yields 4.17 eV, and the experimental measurement[17] is of 4.05 eV. The T_d isomer presents an ionization potential of 4.67 eV, being clearly a manifestation of the great stability with respect to the loss of an electron. The reliability of the calculated ionization potentials has already been shown for the bare lithium clusters.[52]

Figure 3 shows the IR spectra for the Li$_{10}$O cluster; there is a large peak at 326.5 cm^{-1} involving the central oxygen atom and the lithium atoms bonded to it because of the wagging vibration of these atoms.

Figure 4 shows the UV–vis spectra of Li$_{10}$O; as can be seen, there is absorption at the visible region of the spectrum, specifically at 774 nm with oscillator strength of 0.05, corresponding to a transition from singlet to T_2 state. Both spectra can be taken as a prediction and as a way to experimentally confirm the existence of this cluster.

References and Notes

(1) Knight, W. D.; Clemenger, K.; Deheer, W. A.; Saunders, W.; Chou, M. Y.; Cohen, M. L. *Phys. Rev. Lett.* **1984**, *52*, 2141–2143.
(2) Limberger, H. G.; Martin, T. P. *J. Chem. Phys.* **1989**, *90*, 2979–2991.
(3) Fuentealba, P.; Savin, A. *J. Phys. Chem. A* **2001**, *105*, 11531–11533.
(4) Fuentealba, P.; Reyes, O. *J. Phys. Chem. A* **1999**, *103*, 1376–1380.
(5) Ziemann, P. J.; Castleman, A. W. *J. Chem. Phys.* **1991**, *94*, 718–728.
(6) Martin, T. P.; Bergmann, T. *J. Chem. Phys.* **1989**, *90*, 6664–6667.
(7) Wu, C. H.; Kudo, H.; Ihle, H. R. *J. Chem. Phys.* **1979**, *70*, 1815–1820.
(8) Wu, C. H. *Chem. Phys. Lett.* **1987**, *139*, 357–359.
(9) Driess, M.; Pritzkow, H.; Martin, S.; Rell, S.; Fenske, D.; Baum, G. *Angew. Chem., Int. Ed. Engl.* **1996**, *35*, 986–988.
(10) Knapp, C.; Lork, E.; Mews, R. *Z. Anorg. Allg. Chem.* **2003**, *629*, 1511–1514.
(11) Chen, W.; Li, Z. R.; Wu, D.; Li, Y.; Sun, C. C. *J. Chem. Phys.* **2005**, *123*, 164306.
(12) Schleyer, P. V.; Wurthwein, E. U.; Pople, J. A. *J. Am. Chem. Soc.* **1982**, *104*, 5839–5841.
(13) Jones, R. O.; Lichtenstein, A.; Hutter, J. *J. Chem. Phys.* **1997**, *106*, 4566–4574.
(14) Boustani, I.; Pewestorf, W.; Fantucci, P.; Bonacic-Koutecky, V.; Koutecky, J. *Phys. Rev. B* **1987**, *35*, 9437–9450.
(15) Schleyer, P. V. R.; Wuerthwein, E. U.; Kaufmann, E.; Clark, T.; Pople, J. A. *J. Am. Chem. Soc.* **1983**, *105*, 5930–5932.
(16) Lievens, P.; Thoen, P.; Bouckaert, S.; Bouwen, W.; Vanhoutte, F.; Weidele, H.; Silverans, R. E.; Navarro-Vazquez, A.; Schleyer, P. V. *J. Chem. Phys.* **1999**, *110*, 10316–10329.
(17) Viallon, J.; Lebeault, M. A.; Lépine, F. J.; Chevaleyre, J.; Jonin, C.; Allouche, A. R.; Aubert-Frécon, M. *Eur. Phys. J. D* **2005**, *33*, 405–411.
(18) Despa, F.; Bouwen, W.; Vanhoutte, F.; Lievens, P.; Silverans, R. *Eur. Phys. J. D* **2000**, *11*, 403–411.
(19) Centeno, J. *Ph. D. Thesis, in preparation*, Universidad de Chile, 2009.

(20) Johansson, M. P.; Pyykko, P. *Phys. Chem. Chem. Phys.* **2004**, *6*, 2907–2909.

(21) Li, J.; Li, X.; Zhai, H. J.; Wang, L. S. *Science* **2003**, *299*, 864–867.

(22) Zhang, H. F.; Stender, M.; Zhang, R.; Wang, C. M.; Li, J.; Wang, L. S. *J. Phys. Chem. B* **2004**, *108*, 12259–12263.

(23) Zhang, W.; Lu, W.; Sun, J.; Wang, C.; Ho, K. *Chem. Phys. Lett.* **2008**, *455*, 232–237.

(24) Becke, A. D. *J. Chem. Phys.* **1993**, *98*, 5648–5652.

(25) Lee, C.; Yang, W.; Parr, R. G. *Phys. Rev. B* **1988**, *37*, 785.

(26) Vosko, S. H.; Wilk, L.; Nusair, M. *Can. J. Phys.* **1980**, *58*, 1200.

(27) Stephens, P. J.; Devlin, F. J.; Chabalowski, C. F.; Frisch, M. J. *J. Phys. Chem.* **1994**, *98*, 11623–11627.

(28) Krishnan, R.; Binkley, J. S.; Seeger, R.; Pople, J. A. *J. Chem. Phys.* **1980**, *72*, 650–654.

(29) McLean, A. D.; Chandler, G. S. *J. Chem. Phys.* **1980**, *72*, 5639–5648.

(30) Blaudeau, J.; McGrath, M. P.; Curtiss, L. A.; Radom, L. *J. Chem. Phys.* **1997**, *107*, 5016–5021.

(31) Curtiss, L. A.; McGrath, M. P.; Blaudeau, J.; Davis, N. E.; Binning, J.; Radom, L. *J. Chem. Phys.* **1995**, *103*, 6104–6113.

(32) Frisch, M. J.; Pople, J. A.; Binkley, J. S. *J. Chem. Phys.* **1984**, *80*, 3265–3269.

(33) Clark, T.; Chandrasekhar, J.; Spitznagel, G. W.; Schleyer, P. V. R. *J. Comput. Chem.* **1983**, *4*, 294–301.

(34) Frisch, M. J.; Trucks, G. W.; Schlegel, H. B.; Scuseria, G. E.; Robb, M. A.; Cheeseman, J. R.; Montgomery, Jr., J. A.; Vreven, T.; Kudin, K. N.; Buran, J. C.; Millam, J. M.; Iyengar, S. S.; Tomasi, J.; Barone, V.; Mennuncci, B.; Cossi, M.; Scalmani, G.; Rega, N.; Petersson, G. A.; Nakatsuji, H.; Hada, M.; Ehara, M.; Toyota, K.; Fukuda, R.; Hasegawa, J.; Ishida, M.; Nakajima, T.; Honda, Y.; Kitao, O.; Nakai, H.; Klene, M.; Li, X.; Knox, J. E.; Hratchian, H. P.; Cross, J. B.; Bakken, V.; Adamo, C.; Jaramillo, J.; Gomperts, R.; Stratmann, R. E.; Yazyev, O.; Austin, A. J.; Cammi, R.; Pomelli, C.; Ochterski, J. W.; Ayala, P. Y.; Morokuma, K.; Voth, G. A.; Salvador, P.; Dannenberg, J. J.; Zakrzewski, V. G.; Dapprich, S.; Daniels, A. D.; Strain, M. C.; Farkas, O.; Malick, D. K.; Rabuck, A. D.; Raghavachari, K.; Foresman, J. B.; Ortiz, J. V.; Cui, Q.; Baboul, A. G.; Clifford, S.; Cioslowski, J.; Stefanov, B. B.; Liu, G.; Liashenko, A.; Piskorz, P.; Komaromi, I.; Martin, R. L.; Fox, D. J.; Keith, T.; Al-Laham, M. A.; Peng, C. Y.; Nanayakkara, A.; Challacombe, M.; Gill, P. M. W.; Johnson, B.; Chen, W.; Wong, M. W.; Gonzalez, C.; Pople, J. A. *Gaussian 03*; Gaussian, Inc.: Wallingford, CT, 2004.

(35) Glendening, E. D.; Reed, A. E.; Carpenter, J. E.; Weinhold, F. NBO 3.1; NBO 3.1.

(36) Becke, A. D.; Edgecombe, K. E. *J. Chem. Phys.* **1990**, *92*, 5397–5403.

(37) Savin, A.; Becke, A. D.; Flad, J.; Nesper, R.; Preuss, H.; von Schnering, H. G. *Angew. Chem., Int. Ed. Engl.* **1991**, *30*, 409–412.

(38) Silvi, B.; Savin, A. *Nature* **1994**, *371*, 683–686.

(39) Noury, S.; Krokidis, X.; Fuster, F.; Silvi, B. *TopMOD; TopMOD*; Universite Pierre et Marie Curie: France.

(40) Pettersen, E. F.; Goddard, T. D.; Huang, C. C.; Couch, G. S.; Greenblatt, D. M.; Meng, E. C.; Ferrin, T. E. *J. Comput. Chem.* **2004**, *25*, 1605–1612.

(41) DeLano, W. L. *The PyMOL Molecular Graphics System; PyMOL*; DeLano Scientific LLC: San Carlos, CA.

(42) Rousseau, R.; Marx, D. *Chem.—Eur. J.* **2000**, *6*, 2982–2993.

(43) Fuentealba, P.; Chamorro, E.; Santos, J. C. *Understanding and Using the Electron Localization Function in Theoretical Aspects of Chemical Reactivity, 19, 57*; Toro-Labbé, A., Ed.; Elsevier, New York, 2007.

(44) Santos, J.; Andres, J.; Aizman, A.; Fuentealba, P. *J. Chem. Theory Comput.* **2005**, *1*, 83–86.

(45) Leary, R. H. *J. Global Optim.* **1997**, *11*, 35–53.

(46) Bobadova-Parvanova, P.; Jackson, K. A.; Srinivas, S.; Horoi, M.; Kohler, C.; Seifert, G. *J. Chem. Phys.* **2002**, *116*, 3576–3587.

(47) Jackson, K. A.; Horoi, M.; Chaudhuri, I.; Frauenheim, T.; Shvartsburg, A. A. *Phys. Rev. Lett.* **2004**, *93*, 013401.

(48) Yang, M.; Jackson, K. A.; Koehler, C.; Frauenheim, T.; Jellinek, J. *J. Chem. Phys.* **2006**, *124*, 024308–6.

(49) Ahlswede, B.; Jug, K. *J. Comput. Chem.* **1999**, *20*, 563–571.

(50) Jug, K.; Geudtner, G.; Homann, T. *J. Comput. Chem.* **2000**, *21*, 974–987.

(51) Bredow, T.; Geudtner, G.; Jug, K. *J. Comput. Chem.* **2001**, *22*, 861–887.

(52) Florez, E.; Fuentealba, P. *Int. J. Quantum Chem.* **2009**, *109*, 1080–1093.